

Effect of surface and sub-surface infiltration on the behaviour of loose fill slopes

L'effet d'infiltration de surface et sousde surface sur le comportement de desserrés remplis des pentes

Y.D. Zhou, C.Y. Cheuk, K. Xu, L.G. Tham
The University of Hong Kong, Hong Kong, China

ABSTRACT

Based on a field test on a purposely-built loose fill slope, a two-dimensional finite element model is established for coupled hydro-mechanical analyses of slope performance under controlled infiltration conditions. This paper presents a series of parametric study for investigation into the effect of wetting by surface and sub-surface infiltration on the initiation and growth of slope movement as well as the failure mechanism. The simulation results demonstrate that different infiltration schemes can lead to different deformation patterns and in turn influence the onset and propagation of failure. More evidence in the form of cracks development was also observed in the field slope during the controlled wetting test.

RÉSUMÉ

Basé sur une épreuve de terrain sur un exprès construit desserré remplissent la pente, un modèle d'élément fini deux dimensionnelle est établi pour les analyses hydro-mécaniques doubles de performance inclinée dans les conditions d'infiltration contrôlées. Ce papier présente une série d'étude paramétrique pour l'enquête dans l'effet de wetting par l'infiltration de surface et sousde surface sur l'amorce et la croissance de mouvement incliné aussi bien que le mécanisme d'échec. Les résultats de simulation démontrent que de différents projets d'infiltration peuvent causer de différents dessins de déformation et influencer à son tour le commencement et la propagation d'échec. Plus d'évidence se fend sous forme du développement a été aussi observé dans la pente de terrain pendant l'épreuve de wetting contrôlée.

Keywords : Infiltration, surface, sub-surface, loose fill slope

1 INTRODUCTION

Rainfall has been considered as the major cause of many slope failures and landslides in many countries and regions experiencing rainfalls of high intensity. In Hong Kong, many existing old fill slopes were formed prior to 1970s by end-tipping residual soils on natural ground with hardly any proper compaction. Failures of these loose fill slopes under heavy rainfall have posed significant threats and caused severe damage and losses over the past decades (e.g., Lumb 1975; Wong et al. 1998). Yim and Siu (1997) and Wong et al. (1998) have discussed the most common failure modes of loose fill slopes which include static liquefaction, sliding and wash-out. It has been well accepted that generally the performance of an unsaturated soil slope during transient infiltration process depends on the magnitude of the rainfall flux, the soil strength, the coefficient of permeability, the soil-water characteristic curve (SWCC), and the water storage function. Under surface infiltration conditions, the destruction of pore-water suction at a shallow depth has been considered as the most common way through which slope stability is weakened.

Even though much work has been done by many researchers on the effect of infiltration on the behaviour of slopes, the main focus of previous studies was placed on the pore-water pressure response and its effect on slope stability, which is dependent on many intrinsic (coefficient of permeability, soil strength properties, water retention characteristics) or external factors (such as environmental conditions, rainfall pattern and duration). However, not much work can be found on the effect of infiltration water originated from different sources, such as by surface or sub-surface water ingress, on the gradual development of slope movement, as well as possible local and overall failure mechanism.

A field test has been carried out on a purposely-built loose fill slope by the Department of Civil Engineering, the University of Hong Kong (Li 2003). The fill slope is 4.75 m high with an inclination angle of 33°, which is made up of completely decomposed granite (CDG), a silty sand material formed from the weathering process of granites. The total width of the slope was 9 m, with a crest of 4 m width. The initial degree of compaction of the loose fill prior to the field test was ~75% of the maximum dry density measured by standard Proctor test. A variety of loading conditions, including overburden surcharge as well as controlled wetting loads by surface sprinkling and by sub-surface piping infiltration, have been applied during the field test.

Main purpose of the field test is to have an in-depth investigation into the effectiveness of soil nails on strengthening loose fill slopes under surcharge loading and wetting conditions. In this paper the test slope is chosen as a typical case and a coupled hydro-mechanical model is established, in which the nail reinforcement and the surcharge stage are not considered. A series of numerical analyses are carried out for a preliminary study of the effect of surface and sub-surface water infiltration on the development of slope movement and failure mechanism. This paper presents some typical simulation results, and a short comparison is also made with relevant field observations.

2 NUMERICAL APPROACH

The fill soil was taken as a porous medium and modelled by the conventional approach that considered soils as multiphase materials, and a simplified effective stress principle, as shown below, was adopted to describe its behaviour.

$$\bar{\sigma} = \sigma - s u_w \mathbf{I} \quad (1)$$

where $\bar{\sigma}$ and σ are the effective and total stresses respectively; u_w denotes the pore water pressure; s is the saturation degree, and \mathbf{I} is a second-order unit tensor. Darcy's Law was adopted to simulate the pore water flow within soils. More details on the finite element modelling approach can be referred to Zhou et al. (2009).

The middle cross section of the test slope was chosen for a 2-D simplified analysis. As shown in Fig. 1, the test slope was modelled by plane strain 4-node elements with coupled degrees of freedom including pore water pressure and displacements. As a layer of asphalt was applied above the in-situ ground surface as a watertight measure, and the redistribution of water content within the ground soil can be neglected, only deformation variables were incorporated in the ground soil elements. The no-fines concrete layer, as a hard durable coarse free-draining material, was also modelled by finite elements with coupled nodal variables.

The loose fill within the test slope was modelled by an elasto-plastic model denoted as DP/Cap model in this paper, which incorporated a cap yield surface to the extended Drucker-Prager plasticity model (ABAQUS inc. 2006). This elasto-plastic model is capable of providing an inelastic hardening response to account for plastic deformation under compression which was observed in the triaxial tests conducted on local CDG (To et al. 2008). As in most critical state models, nonlinear elasticity was incorporated, and the bulk and shear modulus are defined as a function of the effective mean stress. The yield surfaces consist of a linear Drucker-Prager shear failure surface and a cap surface. A perfect plastic hardening law was assumed for the shear failure surface in the calculations, whilst a power law relating the hydrostatic compression yield stress p'_b and volumetric plastic strain ϵ_{vol}^{in} , was used to define the hardening law for the cap yield surface. Table 1 presents adopted model parameters of CDG soil.

Table 1. Summary of material parameters

| | CDG soil | Ground soil | No-fines concrete |
|----------------------|--|------------------------------|--|
| Basic properties | $\gamma_d=1.41\text{kg/m}^3$, $e_0=0.86$, $M_{c0}=14.9\%$ | - | - |
| Elastic properties | Function ($\kappa=8.4\times 10^{-3}$, $\mu=0.05$) | $E=35\text{MPa}$, $\mu=0.2$ | $E=1\times 10^4\text{MPa}$, $\mu=0.2$ |
| Plastic properties | $d=2\text{kPa}$, $\beta=40^\circ$, $R=0.6$ $p'_b = 29.14e^{21.48\epsilon_{vol}^{in}}$ | - | - |
| Hydraulic properties | Function (Fig. 2) | - | $k=1\times 10^{-4}\text{m/s}$ |

Note: E , M_c , γ_d , e , μ , κ , k are Young's modulus, moisture content, dry density, void ratio, Poisson's ratio, the slope of a recompression-unloading line in the $(1+e)-\ln p'$ space, and permeability coefficient respectively, and the subscript "0" denotes the initial value; d , β and R are respectively the cohesion, friction angle in the $q-p'$ plane, and a parameter that controls the shape of cap surface in DP/Cap model;

The soil-water characteristic curve (SWCC) for the fill soil was extracted from the field measurements. As shown in Fig. 2(a), a unique relationship between matric suction and volumetric moisture content was adopted. The corresponding hydraulic conductivity function for the slope fill was shown in Fig. 2(b) as a function of the saturation degree, which was derived from the SWCC using the technique proposed by Fredlund et al. (1994).

Only linear elastic properties were defined for the ground soil and the no-fines concrete layer under the loose fill, as the possibility of nonlinear deformation within these regions was considered to be quite low. The coefficient of permeability of the no-fines concrete was taken as $1\times 10^{-4}\text{m/s}$, a relatively large value to represent its free-draining property. The full set of parameters for the ground soil and no-fines concrete adopted in the analysis were also summarized in Table 1.

In the numerical model, the displacement boundary conditions were defined as vertical rollers on the left cutting edge, with full fixity at the base and at the toe boundary constrained by the concrete apron (Fig. 1).

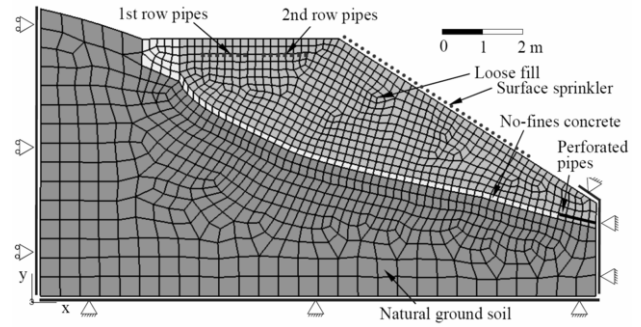
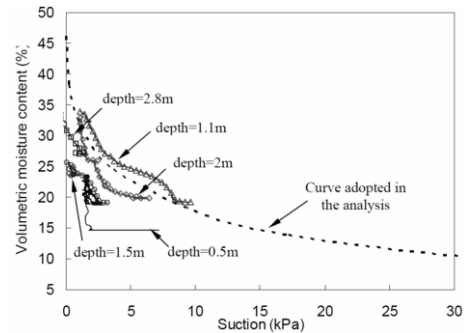
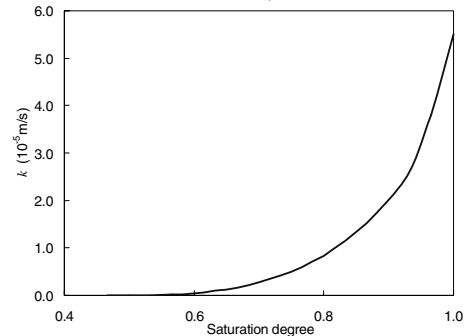


Figure 1. Finite element model of the slope



(a) Soil-water characteristic curve (solid lines denote field data)



(b) Permeability coefficient versus saturation degree

Figure 2. Hydraulic properties of CDG (a~b)

The initial conditions of void ratio as well as the degree of saturation in the fill soil were respectively taken as the averages of field measurements at the beginning of the test. A long-term coupled flow and deformation analysis under the self-weight of the slope fill was first conducted, until a stabilized pore pressure and stress distribution within the slope was obtained, which was then taken as the initial state for the simulation of the subsequent wetting process.

3 PARAMETRIC STUDY

Based on the above model, a series of parametric study was carried out for an investigation into the influence of different infiltration schemes on slope movement and possible sliding failure. Much attention was given to the progressive slope deformation, loss of soil suction as well as mounding of groundwater table relative to the controlled wetting loads in the fill slope. Three infiltration schemes, considering wetting loads originated by surface or sub-surface watering source, were examined in this study. In the first case (Case I), the actual wetting sequence during the field test is modelled, which included both surface sprinkling and buried piping system. In order to study the contribution by each wetting system

separately, two more watering schemes were also simulated, in which only the surface sprinklers' effect (Case II) or the contribution from the sub-surface piping system (Case III) was incorporated. Case II with only surface infiltration water was especially true in built-up areas where the slope crest has been paved, whilst Case III can represent a practical situation when the slope surface is covered by impervious materials, like a chunam cover (Premchitt et al. 1992), and the ingress of water originates from sub-surface locations, such as broken pipes, or geological features. The controlled watering process is shown in Fig. 3, in which the wetting sequence during the first four days was taken to be the same as in the field test, whilst in the subsequent two days, more water ingress was assumed and simulated in order for triggering prominent slope movement.

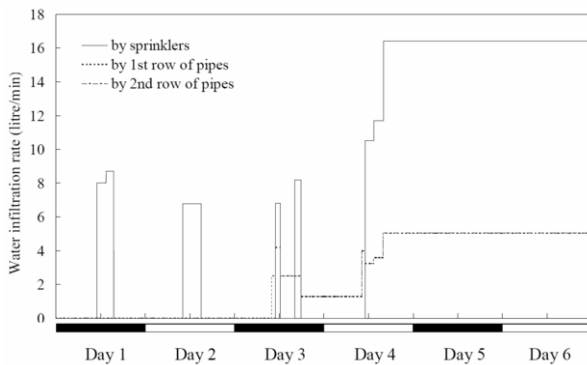


Figure 3. Infiltration rate versus time

4 RESULTS AND DISCUSSIONS

Through a parametric study, some typical simulation results, including the wetting induced slope movement, variation of ground water table (GWT), as well as the initiation and development of plastic deformation within the fill soil are presented below.

Figure 4 presents a comparison of the wetting induced horizontal displacements at a surficial point near the toe apron (Point A) and at the crest corner (Point B), which are vulnerable to slope motion. It can be seen that the slope movements mobilized by the three infiltration schemes are quite different from each other. During the first two days, as only the surface sprinklers were activated for a short term period, only negligibly small movements are obtained in Case I and Case II, whilst no movement is induced in Case III due to the absence of wetting load. During Day 3 and Day 4, relatively larger displacements were mobilized as more infiltration water were supplied by both the surface sprinklers and sub-surface pipes. It can be also seen that under all three wetting schemes, larger horizontal movements were induced at the crest corner than that at Point A, and the sub-surface piping can trigger larger slope movements than the surface sprinkling although the volumes of water provided by each wetting system are basically the same: 12.5m^3 by surface sprinklers, and 12.2m^3 by buried pipes during these two days. During Day 5, the results of Case I illustrate that simultaneous functioning of both surface and sub-surface wetting is capable of triggering abrupt increase of slope deformation, indicating the mobilization of overall sliding failure. However, feeding water by surface sprinkling and sub-surface piping individually (Case II and Case III) only induced a bit increase of horizontal movements at the two points, and the slope stability can be maintained, which is also illustrated by the results of plastic strain distribution below.

The initiation and development of plastic deformation within the slope illustrates the distribution of soil zones in which the strength of soil is insufficient to resist the mobilized stresses. No assumption needs to be made in advance about the location or shape of the failure surface during the coupled flow and

deformation analysis. Based on the simulation results in the designed cases, Figures 5~7 present the development of wetting induced plastic strain magnitude ($\text{PEMAG} = \sqrt{2/3\epsilon^{\text{pl}} : \epsilon^{\text{pl}}}$) within the fill slope at some typical moments during the controlled watering process. The gradual evolution of GWT is also shown for a comparison of the infiltration patterns by different watering schemes.

In general, a comparison of the simulation results in Figs. 5~7 demonstrates that the infiltration scheme plays a significant role in the development of slope movement, infiltration pattern and overall failure mechanism. In Case I, with more infiltration water from both surface and sub-surface wetting systems, relatively higher ground water table is triggered covering the whole bottom surface except a small range close to the slope toe due to the free-drainage conditions there. On late Day 5, the rise of GWT in the lower portion of the fill soil initiated and mobilized a fast development of severe plastic deformation at the toe of the slope. Through continuous wetting, in particular the intense watering during the last two days, a maximum GWT, at a height of $\sim 1.3\text{m}$ above the slope bottom, was mobilized during the final day of wetting. The plastic zone propagated upward and eventually a circular failure zone tangent to the inclined slope base was mobilized within a short period. During the field test, cracks were observed on the slope crest mobilized by the controlled infiltration water by both wetting systems (Li 2003). However, the potential sliding failure was prevented by nails reinforcement.

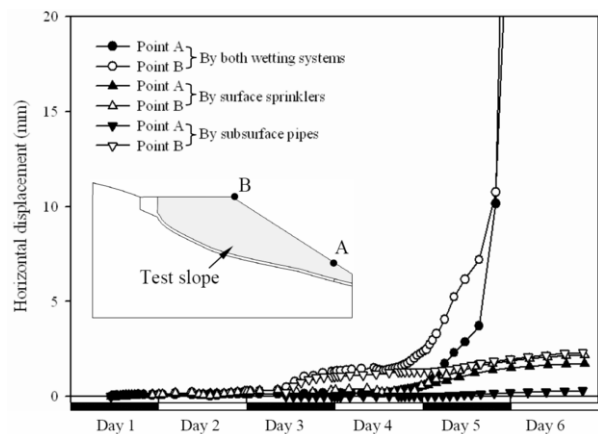


Figure 4. Comparison of wetting induced horizontal displacements by different infiltration schemes

Figures 6 and 7 present the simulation results when the surface and sub-surface wetting systems are activated separately. It can be observed that relatively smaller plastic strain magnitudes were mobilized in these two cases as compared to that in Case I, owing to the fact that less volume of water is infiltrated into the slope in Case II and Case III. Moreover, as shown by the evolutions of GWT in Figs. 6 and 7, different infiltration patterns were induced in the slope, although similar amount of water had been fed into the slope by surface sprinklers and sub-surface pipes separately. In Case II only the part of soil beneath the inclined surface was influenced by the surface wetting, whilst a main portion of deep-seated soil could be affected by the buried piping in Case III. Correspondingly, the wetting induced plastic zones in these two cases present remarkable difference. Interestingly It can be seen that under the surface sprinkling of low intensity during the first 4 days, a shallow zone of plastic deformation was mobilized on late Day 4 (Fig. 6a), even though the whole fill slope remained partially unsaturated, and only a finite zone of soils beneath the sprinkling area were affected by the infiltration water. This observation is in agreement with the field monitored cracks on the inclined surface (Li, 2003), which are approximately at the same location as where the plastic zone outcrops in the vicinity

of the crest corner. In Case III, a plastic zone was first initialized beneath the pipes, and with more water ingress during the last day of wetting, the plastic zone extended downward at a relatively deeper position as compared to the results in Case II. It can be also observed that the plastic zones in Case II and III have not formed a continuous sliding path by the controlled 6-day-long wetting progress, hence the whole slope stability can be maintained in these two cases.

Through a parametric study on the relative significance of hydraulic characteristics of soils on the stability of unsaturated slopes subjected to rainfall infiltration, L'Heureux et al. (2006) pointed out that the different infiltration patterns may lead to different slip surfaces or rupture mechanisms, and in "coarse-grained" soil slopes, the critical surface results from a rotational failure at the toe of slope. The results shown above demonstrate that in sandy soil slope, not only shall a rotational sliding failure starting from the toe of the slope, as depicted by the results in Case I (Fig. 5), be cared for, also some attention shall be paid to possible shallow cracks or sliding when different infiltration schemes can occur in practice. These shallow cracks or local sliding failure due to loss of matric suction can accelerate the infiltration of water and cause a weakening effect on the shear resistance of adjacent soils, which in turn may trigger a more rapid growth of slope movement, or even a global sliding failure.

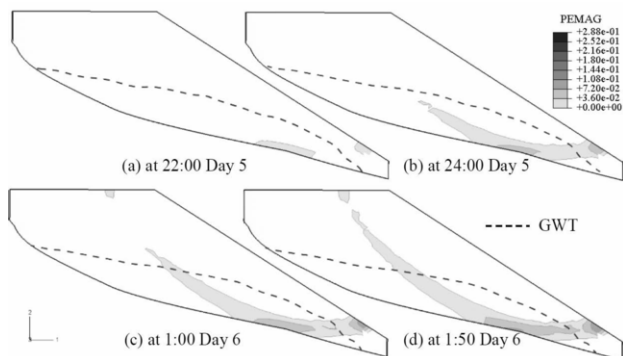


Figure 5. Development of PEMAG by both wetting systems (Case I)

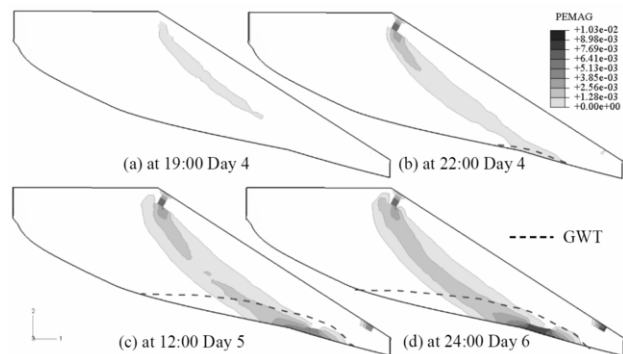


Figure 6. Development of PEMAG by surface sprinklers (Case II)

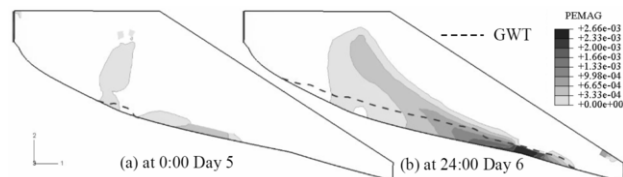


Figure 7. Development of PEMAG by sub-surface pipes (Case III)

5 CONCLUSIONS

Based on a field test carried out on a purposely-built loose fill slope, a 2-D numerical model has been established for coupled pore water flow and soil deformation analysis of slope behaviour under prescribed infiltration conditions. A series of parametric study was undertaken in this paper to study the influence of different wetting schemes, by surface or sub-surface infiltration methods, on the gradual growth of slope deformation, as well as on the initiation and development of plastic zones, which may provide some insights into the wetting induced slope failure mechanism. It is shown by the numerical results that different watering schemes can have a significant effect on the mobilization of slope movement as well as the onset and development of slope failure, as a result of different infiltration patterns triggered. Some evidence was also obtained in the form of cracks growth from field observation during the controlled wetting test on the purposely-built slope. As only a few cases have been discussed in this paper, more analyses based on a more robust numerical model are still needed for an in-depth study of the influence of wetting schemes on unsaturated slope performance.

ACKNOWLEDGEMENT

The authors are grateful for the kind support by Grant No. 7176/05E of the University of Hong Kong.

REFERENCES

- ABAQUS Inc. (2006). Analysis user's manual, Version 6.6.
- Fredlund, D.G., Xing, A.Q., and Huang, S.Y. 1994. Predicting the permeability function for unsaturated soils using the soil-water characteristic curve. *Canadian Geotechnical Journal*, 31: 533-546.
- L'Heureux, J.S.L., Høeg, K. & Høydal, Ø.A. 2006. Numerical analyses and field case study of slope subjected to rainfall. In *Proceedings of the 4th international conference on unsaturated soils*. April 2006, Carefree, Arizona.
- Li, J. 2003. Field study of a soil nailed loose fill slope. Ph.D. Thesis, The University of Hong Kong, Hong Kong.
- Lumb, P. 1975. Slope Failures in Hong Kong, *Quarterly Journal of Engineering Geology*, 8: 31-65.
- Premchitt, J. Lam, T.S.K. Shen, J.M. et al. 1992. Rainstorm runoff on slopes. GEO Report No. 12. Geotechnical Engineering Office, Hong Kong Government, Hong Kong.
- To, E.C.Y. Tham, L.G. & Zhou, Y.D. 2008. An elasto-plastic model for saturated loosely compacted completely decomposed granite, *Geomechanics and Geoengineering*, 3(1): 13-25.
- Wong, H.N. Ho, K.K.S. Pun, W.K. et al. 1998. Observations from Some Landslide Studies in Hong Kong. In *Slope Engineering in Hong Kong*. Balkema, Rotterdam, pp. 277-286.
- Yim, K.P. & Siu, C.K. 1997. Stability investigation and preventive works design for old fill slopes. In *Hong Kong, Proceeding of the 16th HKIE Geotechnical Annual Seminar*, Balkema. 295-302.
- Zhou, Y.D. Cheuk, C.Y. & Tham, L.G. 2009. Numerical modelling of soil nails in loose fill slope under surcharge loading. *Comput & Geotech.*, doi:10.1016/j.compgeo.2009.01.010.